INVESTIGATION OF MAGNETIC DOMAIN STRUCTURE

IN SINGLE CRYSTAL GARNETS

by

ERNEST JOHN SCHEYDER

COURSE XIII-A

MAY, 1964

INVESTIGATION OF MAGNETIC DOMAIN STRUCTURE

IN SINGLE CRYSTAL GARNETS

by

ERNEST JOHN SCHEYDER

B.S., United States Naval Academy
(1956)

SUBMITTED IN PARTIAL FULFILLMENT OF THE

REQUIREMENTS FOR THE DEGREE OF

NAVAL ENGINEER

AND THE DEGREE OF

MASTER OF SCIENCE

IN

ELECTRICAL ENGINEERING

AT THE

MASSACHUSETTS INSTITUTE OF TECHNOLOGY
June, 1964

INVESTIGATION OF MAGNETIC DOMAIN STRUCTURE

IN SINGLE CRYSTAL GARNETS

by

ERNEST JOHN SCHEYDER

ABSTRACT

Magnetic domain structures in carefully prepared samples of
single crystal ferrimagnetic yttrium iron garnet are observable
under a microscope using colloidal suspension techniques. These
samples are subjected to different magnetic fields and the
influence of such external fields on magnetic domain structure
are observed and reported on. Correlation between the observed
structures and theoretically predicted structures is made.

Sample preparation techniques including orientation, mounting,
polishing methods, and etching results are reported.

Attempts at domain observation using dry powder techniques
are described.

Thesis Supervisor: David J. Epstein
Title: Professor of Electrical Engineering

ACKNOWLEDGEMENT

TABLE OF CONTENTS

LIST OF FIGURES

CHAPTER I

INTRODUCTION

This paper devotes itself to an experimental study of magnetic domain structures in carefully prepared samples of single crystal garnets. Rectangular shaped specimens of pure yttrium-iron garnet are subjected to different magnetic fields. Using the versatile Bitter pattern (1)* technique, the resulting domain structures are visually studied.

The organization of this paper falls into four major areas. There is a brief discussion of domain theory in general, followed by a discussion of the experiment and its results. The next section deals with how the observed phenomena correlate with theoretical considerations. The final section discusses miscellaneous experimental results and suggestions for further work in this field.

---

* Numbers inside parenthesis refer to references listed in Appendix D.

CHAPTER II

MAGNETISM AND DOMAIN THEORY

2.1 Source of Magnetism

The contributions of many theoreticians and experimentalists together with the close correlation of their ideas and data confirm the fact that the fundamental source of observed magnetic phenomena in a given crystal is the mutual interaction of the magnetic moments experienced by certain of its electrons. The relative degree of intensity of magnetization or the amount of external macroscopic measurable magnetization in a crystal depends on the arrangement or orderliness of the directions of these magnetic moments.

A system in which the directions of the electron magnetic moments are arranged randomly throughout the crystal and whose magnetic moments are free and independent to the extent that there are no important mutual interactions between magnetic moments, is called paramagnetic.

Other systems exist in which there is a marked mutual interaction between the electron magnetic moments in the crystal. If the mutual interaction is the result of a parallel alignment of the magnetic moments of the electrons, the system is called ferromagnetic. If the mutual interaction arises from the magnetic moments aligning anti-parallel to one another, the system is called ferrimagnetic or anti-ferromagnetic.

In paramagnetic systems, the overriding forces are of a thermal nature. The magnetic behavior of such systems when stimulated by the application of an external magnetic field is only slightly influenced. Ferrimagnetic and ferromagnetic systems, on the other hand, are easily stimulated by the application of even small magnetic fields (<1 oer).

The predominant forces within these systems arise from the mutual interactions of the magnetic moments and, below a certain critical temperature, override the ever present thermally excited forces.

2.2 The Domain Hypothesis

The problem that faced many investigators was to account for the differences between paramagnetic and ferro or ferrimagnetic systems. The result of the work of many contributors is what has come to be called the "Domain Hypothesis." In distilled form it states essentially that:

1. At the absolute zero of temperature all the magnetic moments in a crystal are aligned in the same direction. With increasing temperatures the spin directions deviate from the original direction, doing so until a certain critical temperature, referred to as the Curie temperature in a ferromagnetic material and as the Néel temperature in a ferrite, is reached. Above this temperature the spin directions are random, free, and mutually independent. The material behaves paramagnetically.

2. The above condition is localized, occurring in small areas of the crystal. Such small areas are called magnetic domains. The net magnetic moment present within each domain is referred to as the spontaneous magnetization and is hereafter defined as I_s.

The domain hypothesis therefore permits the net magnetization of a crystal to have any value from zero, if the net magnetic moment is zero, to a saturation value equal to the spontaneous magnetization of each localized zone or domain, if all domains are magnetized in the same direction.

As previously stated, a ferrimagnetic material is one whose net magnetic moment arises from an anti-parallel spin interaction. These ideas concerning negative interaction phenomena were first suggested by Néel in 1948 (2). Originally, the domain theory was developed to describe ferromagnetic phenomena. However, since the domain model utilizes the macroscopic or externally observable properties of a magnetic system, it can also adequately describe the domain structure in ferrimagnetic media even though the source of the domain magnetization is different.

In magnetic crystals there is a tendency for the spontaneous magnetization to lie in one of a small number of so-called easy or preferred directions. Neighboring domains are magnetized in one of these easy directions and are separated by transition zones known as Bloch or domain walls. These Bloch walls are typically on the order of 10^{-5} cm in width. (3) The character of the wall depends on the angular rotation suffered by the domain magnetization as it moves from one domain across the wall and into the next domain.

2.3 Energy Considerations and Domain Structure

The existing domain structure in a magnetic crystal is strongly influenced by the energy in the multidomain system and the shape of the crystal. From an energy point of view, the domain geometry must correspond to the minimum energy state of this multi-domain system. Therefore a short discussion of the more likely energy terms to be included in any analysis of a magnetic system is in order.

2.4 Magnetocrystalline Anisotropy Energy

Since the domain magnetization in a crystal prefers certain easy directions, an anisotropy energy can be expressed phenomenologically as a power series expansion in terms of the direction cosines α_1, α_2 and α_3 of the spontaneous magnetization relative to the principal axes of the crystal(4). For cubic crystals, data can be fitted well when the measurable constants K_o, K_1 and K_2 are used in the following manner:

$$E_K = K_o + K_1 (\alpha_1{}^2 \alpha_2{}^2 + \alpha_1{}^2 \alpha_3{}^2 + \alpha_2{}^2 \alpha_3{}^2)$$
$$+ K_2 (\alpha_1{}^2 \alpha_2{}^2 \alpha_3{}^2) + \ldots$$

K_o is an isotropic term and therefore serves only as an energy reference level; K_2 is normally $\ll K_1$. Therefore the anisotropy energy is expressable as:

$$E_K = K_1 (\alpha_1{}^2 \alpha_2{}^2 + \alpha_1{}^2 \alpha_3{}^2 + \alpha_2{}^2 \alpha_3{}^2) \text{ergs/cm}^3$$

2.5 Energy Contribution of an Applied Magnetic Field

When an external field H is applied in a direction making an angle Θ with the domain magnetization, its contribution to the energy of the system is:

$$E_H = -I_s H \cos \Theta \quad \text{ergs/cc}$$

where I_s is the domain spontaneous magnetization.

2.6 Magnetostrictive Energy

A crystal that is subjected to external stress or one that contains unrelieved strains will have an associated stress energy term. This energy represents the work done against external stress or strains and is accompanied by a change in the physical dimensions of the

material as the direction of the domain magnetization is changed. This
energy term will not be used in this experiment and is mentioned here
for information only.

2.7 Magnetostatic Energy

This term describes the energy of the demagnetizing field and
results from the presence of exposed poles in the crystal. It is
therefore extremely dependent on the geometric configuration of the
sample. Numerically, it is equal to $E_M = \frac{1}{2} N I_s^2$, where N is a
demagnetizing coefficient. Kittel (5) discusses magnetostatic energy
terms for a variety of shapes and geometries.

2.8 Wall Energy

Domain walls have finite size and represent a transition zone
between adjacent domains in which the spin directions change as the
magnetization vector moves from one domain to the next. Consequently,
they require energy for their formation. Néel (6) and others have
developed analytical expressions to describe the energy densities
of walls having different orientations with respect to the principal
crystallographic directions, and will be referred to later in the
paper.

The above listed energy terms constitute the major contributions
to domain energy and their sum represents the total energy density
in a crystal. Accordingly, the domain configuration which minimizes
this total energy is the domain geometry that will exist within the
crystal.

CHAPTER III

OBSERVATION OF DOMAINS

Although there are several available methods for observing magnetic domain structures, (7) the most often used and most versatile is that employing magnetic powder patterns as developed by Bitter,(1) Elmore (8) and others. A thin layer of liquid in which fine ($< 1.0\mu$) magnetic particles are held in colloidal suspension is applied to a sample whose surface has been specially prepared. Appendix A gives a detailed description of the colloid preparation process. Variations in the magnetic field across the Bloch walls in the sample result in concentrations of the colloid along the edges of these walls. Kittel (5) discusses the phenomena in detail. These colloid groupings provide visible evidence of a Bloch wall and are readily observed at moderate magnification (< 100 x) with ordinary optical microscopes. Bloch wall motions caused by controlled variations of an applied magnetic field are also clearly visible.

CHAPTER IV

EXPERIMENTAL PROCEDURE

4.1 Sample Orientation

Single crystals of pure yttrium-iron garnet hereafter referred to
as YIG, were grown by Mr. R. Hunt at the Laboratory for Insulation
Research, M.I.T., Cambridge, Mass. Appendix B describes the crystal
growing process. Using standard crystal X-ray orientation techniques
(9), the (110) plane of the garnet was located. Samples approximately
0.012 to 0.015 inches in thickness with surfaces parallel to the
(110) plane were cut. These samples proved satisfactory but because
of experience gained during subsequent cutting and polishing, samples
cut thicker ($\approx$ 0.050") would have been better. These flat (110) plane
thin discs were again X-ray oriented and the [110] direction located.
Rectangular samples were cut whose long edges were parallel to the
[110] direction, as illustrated in figure 1(a).

The rectangular shape was selected because of the simplifications
such a geometry introduce into the theory used to describe its domain
structure. Rectangular samples were also easy to fabricate.

As discussed earlier, there is a demagnetizing energy associated
with domain structure due to the presence of exposed poles. A
magnetized toroid would theoretically contain no exposed poles.
Accordingly, a toroid, cut in the (110) plane, was also prepared.

For YIG the preferred direction of magnetization in the (110)
plane is the [111] direction as illustrated in figure 1(b). The
rectangular specimen used was 5.6 mm long, 0.88 mm wide and had a
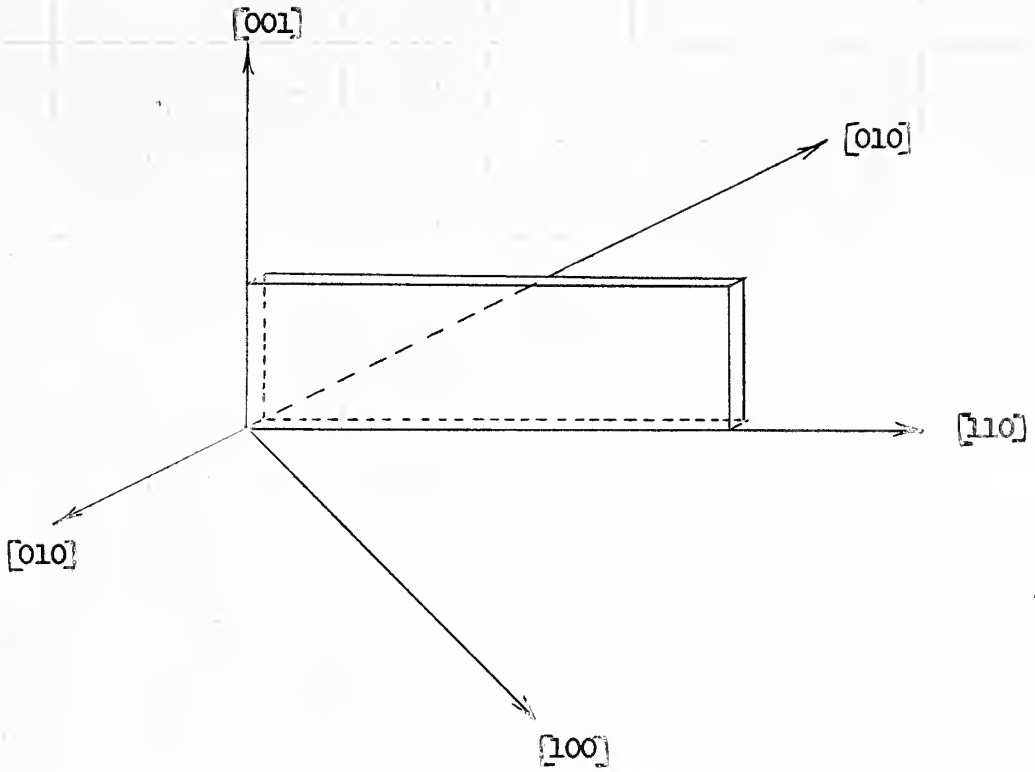thickness of 0.20 mm.

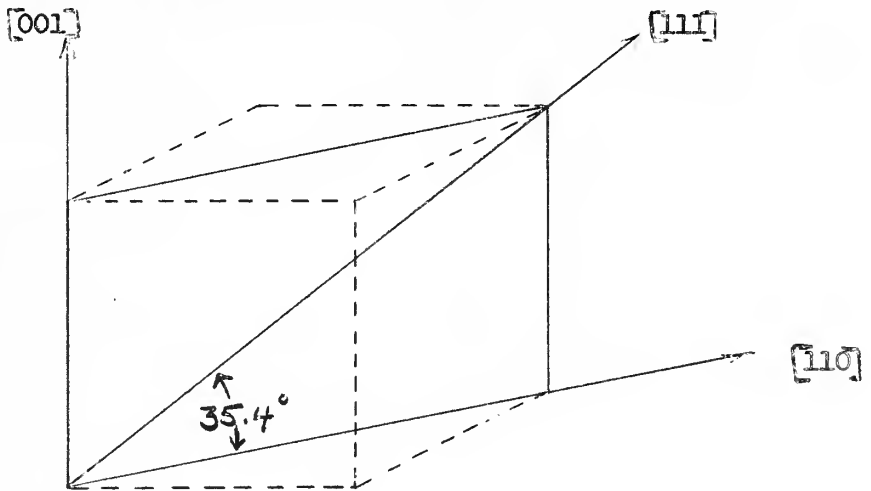Figure 1(a) - Crystallographic orientation of samples.

Figure 1(b) - Preferred direction of magnetization for YIG

is $[111]$ direction.

4.2 Sample Polishing

Because of the critical influence it has on the polishing process,
a short discussion of sample mounting methods is in order. Two types
of adhesives were used, liquid Canada balsam and solid Canada balsam.
Experimental experience clearly showed a marked preference. Solid
balsam was found superior mainly because the liquid balsam required
up to 24 hours to dry and harden completely. Therefore only the
solid balsam adhesive mounting method will be discussed .

As stated in Chapter III, a well prepared surface is needed before
magnetic domains may be observed by colloidal techniques. For
polishing purposes, the samples were mounted on circular phenolic blocks,
two inches in diameter and one inch thick. The blocks were preheated
to approximately $125^{\circ}C$ and enough solid balsam was melted onto the
block's surface to hold the specimen firmly in place. Because it was
essential that the (110) plane be preserved throughout the polishing
process, three or more samples from the same cutting batch were
mounted on the same polishing block. This method maintained the
(110) plane to within $1/2^{\circ}$ in each sample.

The actual preparation of the sample surface was perhaps the
most time consuming and tedious portion of the experiment. Of the
several procedures tried, one polishing method evolved which produced
the most satisfactory specimen surfaces.

One important feature is considered most critical for any kind of
successful polishing regardless of method. Extraordinary effort must
be made to insure that small pieces of the crystal do not chip off the
edges of the sample and subsequently scratch the surface while one is
polishing. This problem was encountered repeatedly, but was finally

solved by two corrective measures:

1. The edges were beveled to the point where there was
    curvature sufficient to prevent chipping.

2. The edges were immersed in excess balsam during the mounting
    process. With subsequent polishing, both balsam and
    sample were polished together.

Once the samples were adequately mounted, the polishing procedure
that followed was quite simple. Polishing may be done mechanically
or manually. Early attempts using glass and phenolic flats produced
scratched surfaces. It became apparent that when polishing pastes
smaller than 100 microns were used, the polishing had to be done on
cloth covered flats (preferably of silk), if a satisfactory surface
was to be gotten. Finer and finer polishing compounds were used until
the desired finish was obtained. Between compound changes, however,
the sample was checked optically to insure that the previous grit had
removed all scratches larger than its own size. A recommended abrasive
schedule for obtaining an optically satisfactory surface for domain
observation in YIG is given below.

Polish Time	Polish Compound
1/2 to 1 min.	320 paper
1/2 to 1 min.	600 paper
2 to 5 mins.	A.O. 305 on glass flat
15 min. +	40 micron diamond paste in silk covered glass flat
15 min. +	3 micron diamond paste on silk covered glass flat
15 min. +	3/4 micron Linde A polishing compound on silk covered glass flat
30 min. +	0.30 micron Linde B polishing compound on silk covered glass flat

4.3 <u>Etching Experiments</u>

Etchants of 50% by volume of concentrated HCl and water, and 50% by volume of concentrated HNO_3 and water were used on the polished crystals. Other workers have reported that these etchants relieved polish induced strains in the sample surface. This experimenter's etching results were disastrous. Samples were etched at approximately $90^{\circ}C$ for from ten to thirty minutes. The general etching result was pitting of the surface to the point where repolishing became necessary.

It was subsequently discovered that by using the polishing process described herein, a strain free surface could be produced in the YIG samples. The photographic results of this experiment, presented in a later section, attest to this fact in that none of the maze type domain patterns so typical of strained surfaces is present.

4.4 <u>Sample Observation</u>

The polished sample was next mounted on a glass slide and made ready for optical examination. A Zeiss binocular optical microscope with magnifications up to 150 x was used. Indirect illumination, as suggested by Williams, Bozorth and Shockley (10) to sharpen the appearance of the Bloch walls was also utilized. A 3/4" thin glass cover slide supported by mounting wax was placed over the sample and a droplet of colloid was placed between the sample and the cover slide.

Figure 2 is a photograph of the domain structure to be found in a rectangular shaped sample of YIG oriented as shown in the (110) plane. A comparison of figures 1 and 2, shows that [111] is the easy direction of magnetization for YIG in the (110) plane. As
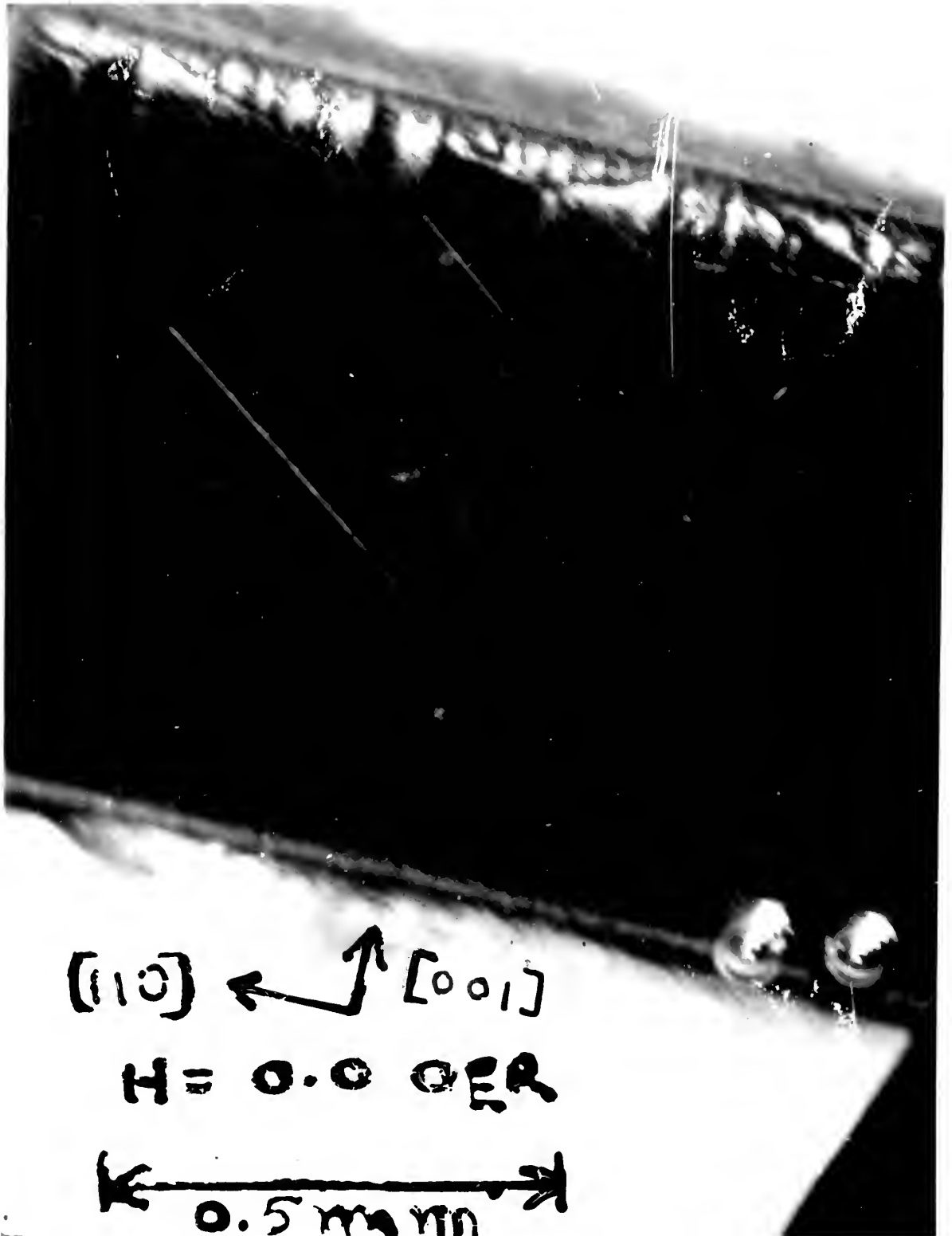
[110] ← ↑ [001]

H = 0.0 OER

|← 0.5 mm →|

FIGURE 2.

expected in crystals having [111] as their easy direction of magnetiza-
tion, 180°, 109° and 71° type Bloch walls are present. Figure 2 also
shows how the thickness of these Bloch walls is a function of the angle
through which the domain magnetization vector must rotate in going
from one domain to another. The relationship between this angle of
rotation and the wall energy as developed by Néel (6), is used in a
later section.

Yamamoto and Iwata (11) and Williams and Walker (12) reported the
same type domain structures in the (110) plane of nickle which also has
[111] as its easy direction of magnetization.

4.5 Influence of an Applied Magnetic Field

The rectangular specimen of YIG was next mounted between the poles
of an electromagnet in order to study the effects of variations of
applied magnetic field on domain structure. The magnetic field was
applied parallel to the long direction [110] of the sample. Figure 3
illustrates the experimental setup. A gaussmeter having a range of
0 to 400 gauss, was mounted permanently, thus providing direct measurement
of the applied field at any instant. The Zeiss microscope was mounted
in a specially prepared jig as was the Polaroid Land camera. Type 42
film having a speed of 200 x was employed.

The sample was demagnetized by subjecting it to full field reversals
of decreasing strength until zero field was reached. The field was
then increased in small increments until the sample became essentially
saturated. Attention was focused on the higher field responses of the
system ($10 < H < 70$ oersteds). Figures 4, 5 and 6 illustrate the effects
of applied magnetic field variations on the magnetic domain structures
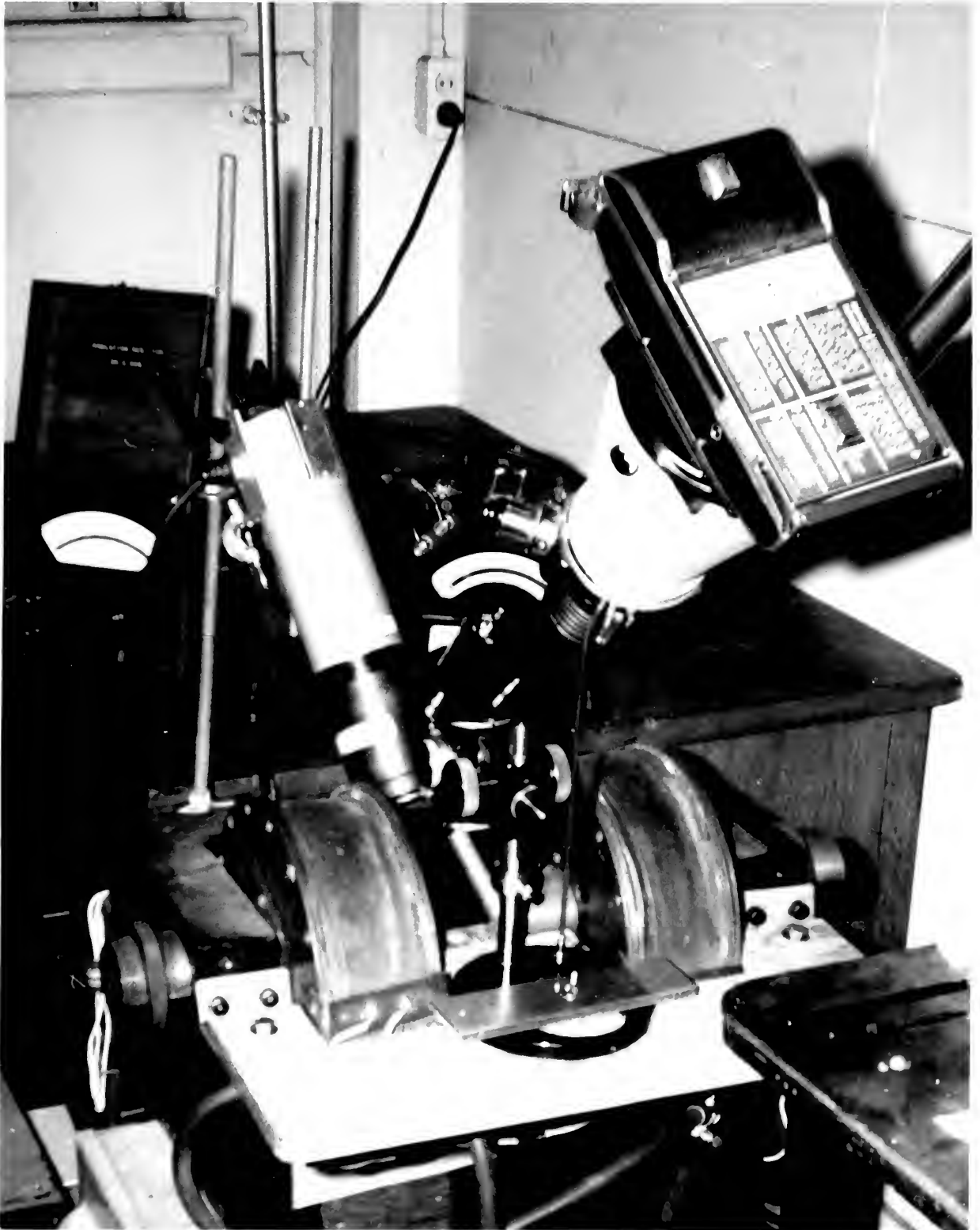
FIGURE 3.

in the YIG. The following conclusions have been reached from a study of the photographic evidence:

1. As the applied field was increased, the Bloch walls aligned themselves normal to the long dimension of the rod and gradually moved toward each other.

2. At moderate fields ($\approx$ 20 oe.) the domain closure patterns at the long edges of the sample were of a type predicted by Néel. (6)

3. As the field was increased, the concentration of colloid at the opposite short edges of the rectangular specimen increased. This intimated the creation of poles and therefore concentrations of magnetostatic energy at the ends of the sample.

4. The ribbon-like structure of the Bloch walls appeared essentially in the central bulk of the sample. The domain structures at the ends (near the created poles of 3 above) appeared confused.

5. The bulk of the sample became saturated when the applied field was approximately 40 oersteds.

Figure 7 is a plot of the observed variation of domain wall spacing in the bulk of the material with the observed applied magnetic field. It shows that the wall spacings gradually decrease until a point is reached where they remain essentially constant. At this point the domain magnetizations are all in the same direction and the crystal is considered saturated.
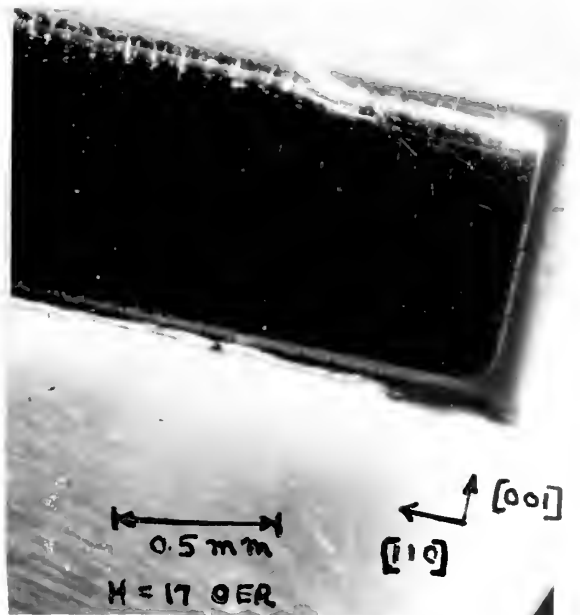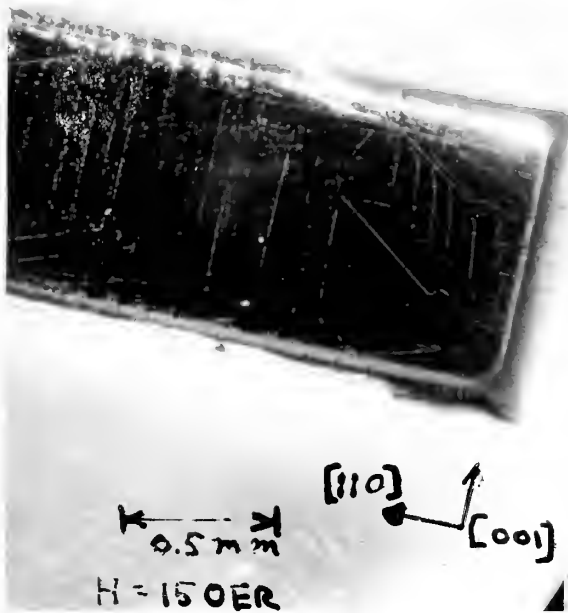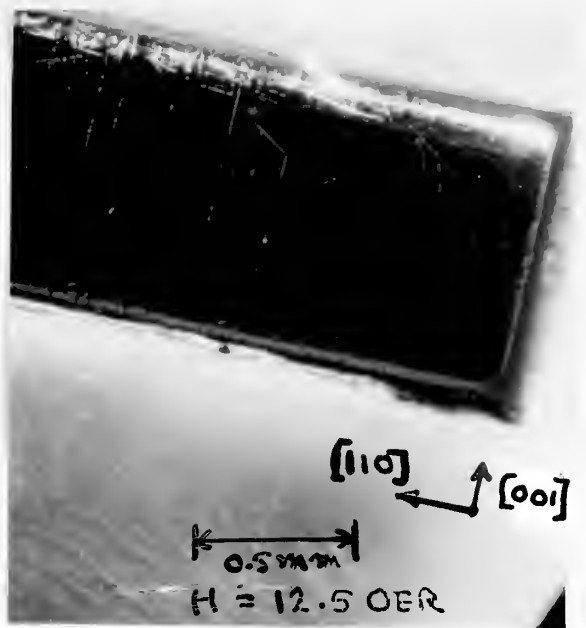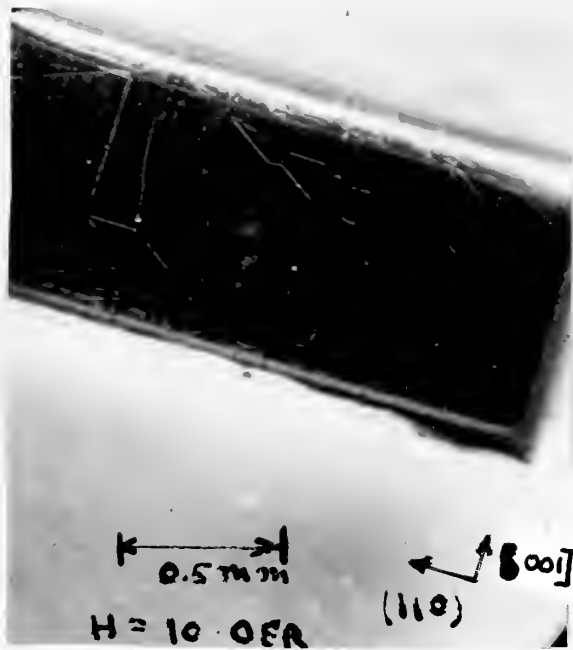
Figure 4.

0.5mm [110] ↑[001]

H = 20 OER

0.5mm [110] ↑[001]

H - 22 OER

0.5 mm [110] ↑[001]

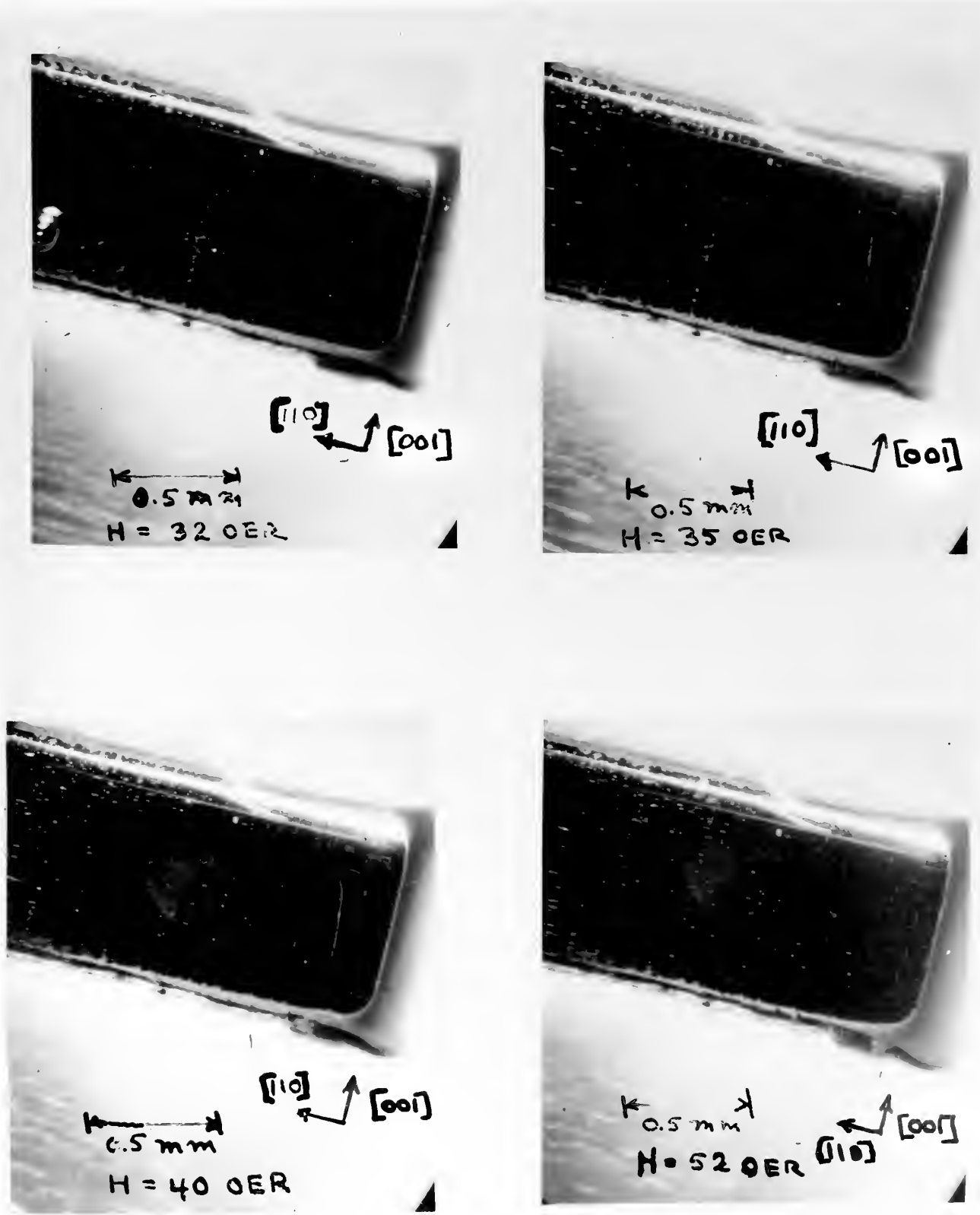H = 25 OER

[110] ↑[001]

0.5 mm
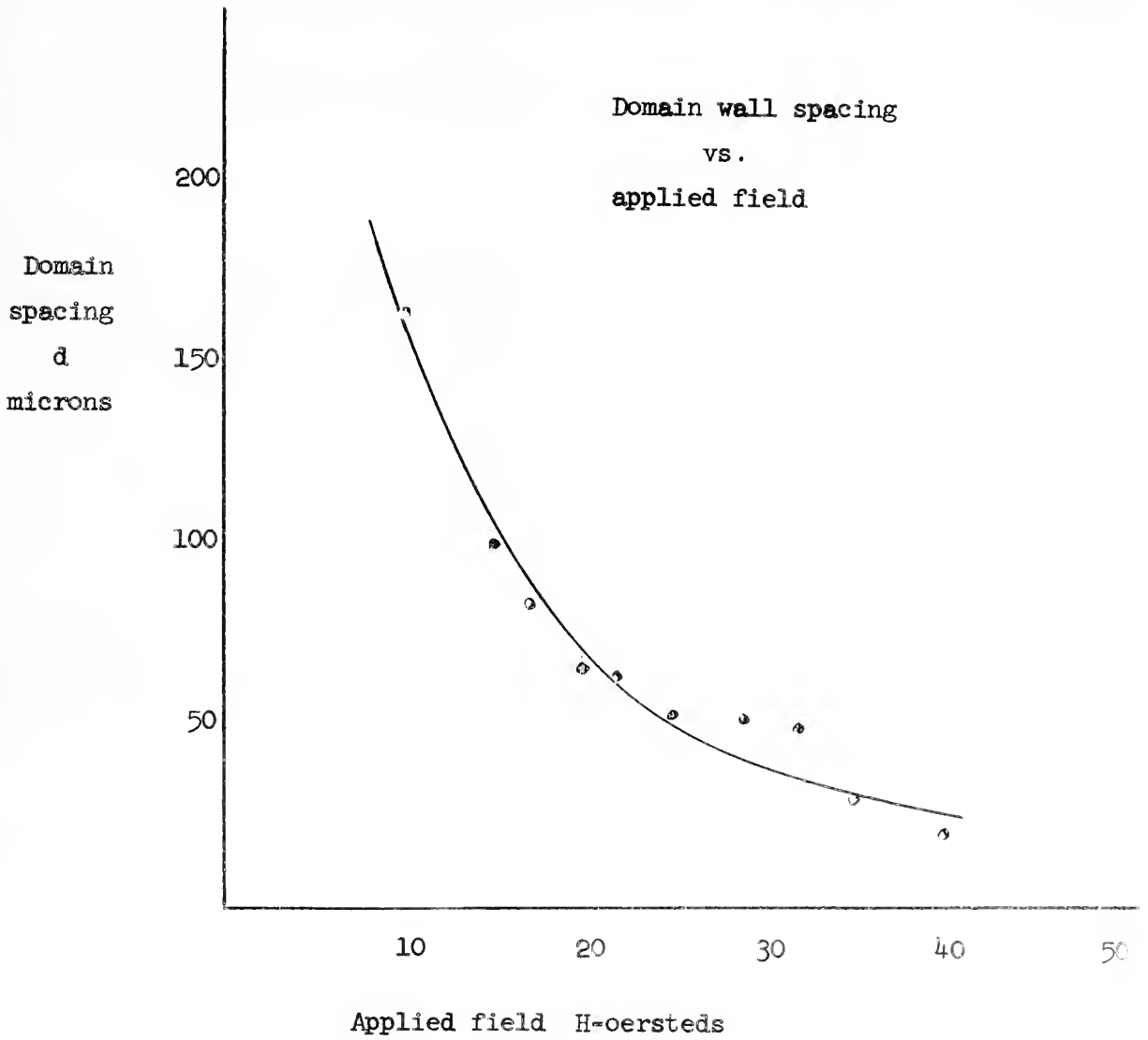
H = 29 OER

Figure 6.

Figure 7 - Plot of observed domain spacing vs. applied field
strength.

CHAPTER V

COMPARISON WITH THEORY

5.1 System Model

It has been shown by Néel (2,6), Kittel (5,12), Stewart (3) and many others that subdivision into domains arises from a need to minimize the demagnetizing field in the crystal. Also, in order to prevent large demagnetizing fields near domain boundaries, the density of free poles along these boundaries must be small. These constraints therefore determine to a large extent the general shape of the domains. The (110) plane rectangular specimen used in this experiment was subjected to a small external magnetic field in the $[110]$ direction. Both sample shape and applied field acted to force the domain magnetizations to be equally distributed between the two preferred directions nearest the applied magnetic field. The additional constraint that free poles must not appear at the domain boundaries forced the main domain structure in the bulk of the sample to be arranged as in figure 8(a). Kittel (5) has shown that the domain structure of figure 8(a) exists only in media in which $\dfrac{K_1}{I_s^2} > 1$. For YIG, $\dfrac{K_1}{I_s^2} = 0.28$.

Landau and Lifshitz, Néel and Kittel, among many, have proposed various type closure patterns that close the flux of the main domain structure and thereby modify figure 8(a). Figures 8(b) and 8(c) are possible closure configurations for this sample.

The type of closure pattern has a strong influence on the resulting domain spacing. The domain spacing that finally exists is one corresponding to the minimum energy required to form a Bloch wall and a closure.
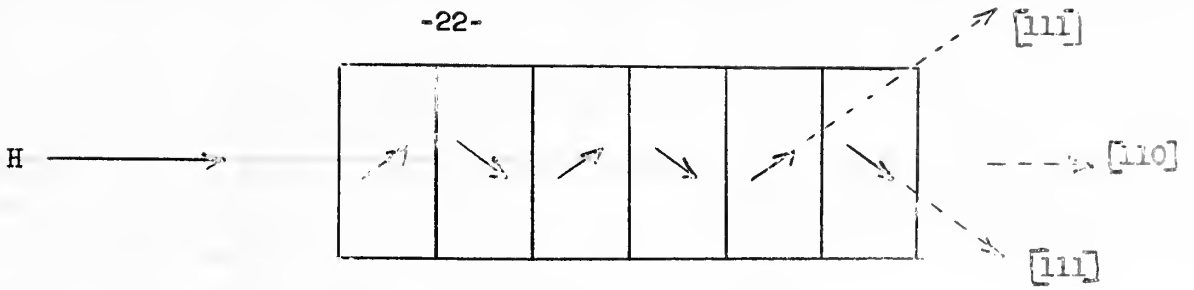
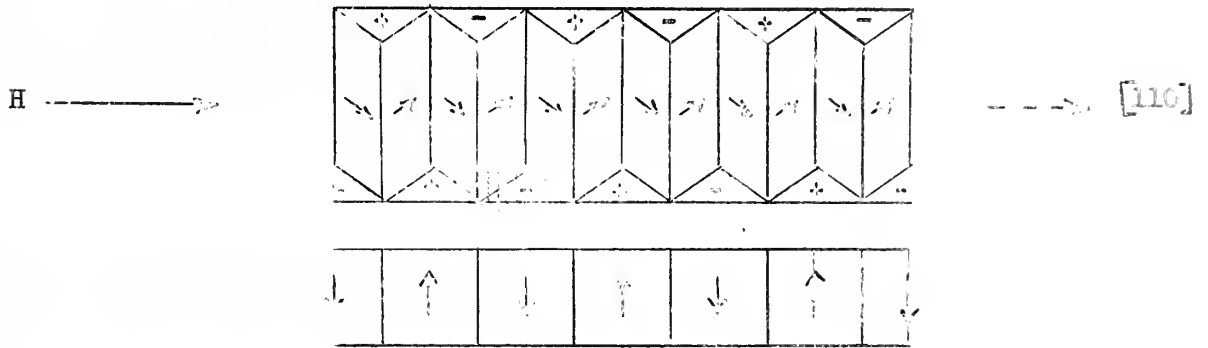Figure 8(a) - Arrangement of main domains in YIG sample.
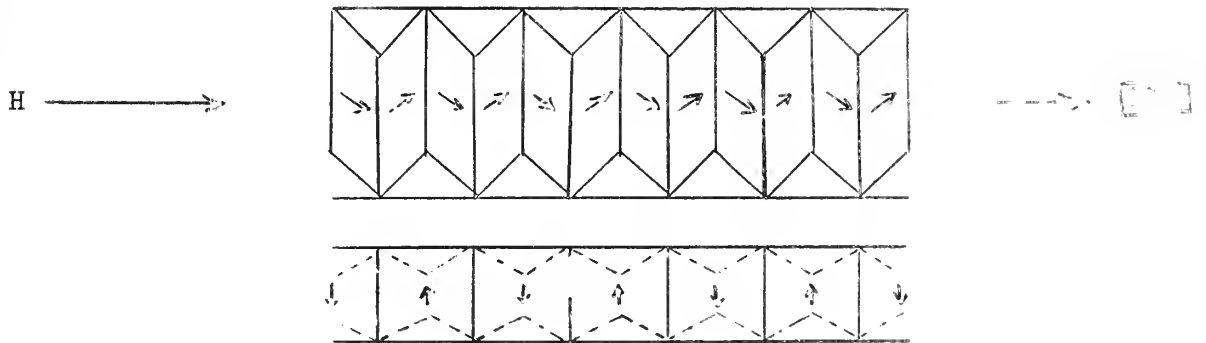

Figure 8(b) - Pattern with closure domains.

Figure 8(c) - More complicated closure structures at upper and
lower surface eliminates free pole effect.

In Appendix C, an expression for the wall energy γ is developed. Defining the excess energy in a closure per unit pattern length as W_x, the excess energy in the wall and closure above the energy in the bulk of the sample can be computed as,

$$W_{excess} = \frac{\gamma L}{d} + W_x = \frac{\gamma L}{d} + f(d)$$

W_x is a function of wall spacing and the type of closure actually present. For the condition that this energy be a minimum, $\dfrac{dW_{excess}}{d(d)} = 0$ and $\dfrac{\gamma L}{d} + f'(d) = 0$. It is evident that the quantity $f'(d)$ has a strong influence on the final value of domain spacing and in turn its value is directly controlled by the closure pattern actually existing in the crystal.

Figures 8(b) and 8(c) illustrate two possible closure patterns that could exist in the crystal. Similar type closures are visible in the photographs presented in Chapter 4. The pattern of figure 8(b) is not a completely closed one because free poles are produced at the top and bottom of the sample. The energy associated with these free poles can theoretically be reduced by a change in the closure pattern at the surface. The more complicated structure of figure 8(c) is a possible pattern that reduces this free pole effect.

Closures of the type illustrated in figure 8(b) are used in the subsequent theoretical treatment of the problem. The pattern of figure 8(c), though probably much closer to the actual structures observed, lead to cumbersome algebraic expressions which add little to the basic understanding of the phenomena. In closures of figure 8(b), magnetocrystalline energy and magnetostatic energy terms are the only

contributors to the energy within the closure. Furthermore, the ratio of magnetostatic to magnetocrystalline energy is small and varies as the ratio of domain spacing to sample thickness[5], i.e. $\dfrac{E_m}{E_K}\bigg|_{closure} = c\,\dfrac{d}{t}$;

d = domain spacing, t = sample thickness, c = geometry factor. For the sample used, $c \cong 1$ and $\dfrac{d}{t} = 0.1$. The approximation is therefore made that the magnetostatic energy may be ignored.

5.2 Theoretical Domain Spacing

Using the expressions for the various energies introduced in Chapter II, the calculation of the excess energy in the closures and the wall energy is possible. Figure 9 illustrates the geometry of the problem. The detailed algebraic manipulations are carried out in Appendix C.

In the bulk of the sample, the energy is equal to:

$$E_{bulk} = E_K + E_H$$

where E_K and E_H are both expressable as functions of the angle Θ, the angle between the domain magnetization and the applied field. Energy minimization procedures on this expression lead to the following results. From Appendix C:

$$H = \frac{K_1}{I_s}\ \cos\Theta\ (3\sin^2\Theta - 1)$$

$$E_{bulk} = \frac{K_1}{4}\ (15 - 14\sin^2\Theta + 9\sin^4\Theta)$$

The excess energy in the domain closure of figure 8(b) above that in the bulk is defined as E_b. In the closure, $E_{K_b} = \dfrac{K_1}{4}$ and $E_{H_b} = 0$ and therefore,

$$E_{closure} = E_{K_b} + E_{H_b} = E_{bulk} + E_b$$
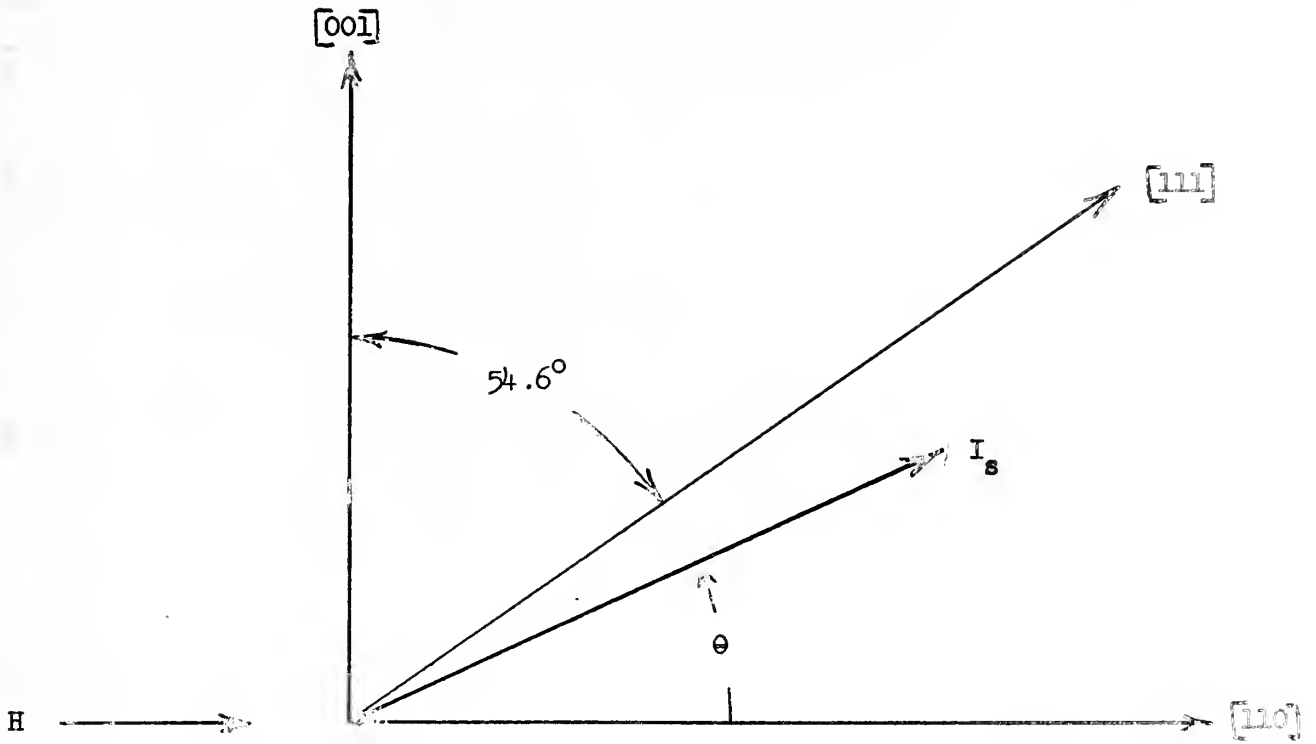
Figure 9 - Direction of domain magnetization with field applied
in [110] direction.

Solving for E_b leads to the result that

$$E_b = - K_1 + \frac{K_1}{4} \sin^2 \theta (14 - 9 \sin^2 \theta)$$

From the geometry of the closure pattern in figure 8(b), the excess energy per unit pattern length d is:

$$W_x = d^2 \frac{E_b}{4} \tan \theta = d^2 W_b$$

$$\text{where} \quad W_b = \frac{E_b}{4} \tan \theta.$$

Knowing the wall energy density γ , (Appendix C), and the excess energy in the closure, the total energy above bulk energy needed to form a wall and a closure per unit of pattern length d is:

$$W_S = \frac{1}{d} \ d^2 \ W_b \ + \ \frac{\gamma L}{d}$$

The value of d that minimizes this expression is found by setting $\frac{dW_S}{d(d)} = 0$

$$d = \sqrt{\frac{\gamma L}{W_b}}$$

TABLE I

θ	H oersted	W_b ergs/cm^3	γ ergs/cm^2	d microns
33	3.1	143	25.4×10^{-3}	40
30	8.5	210	23.2	31.2
25	16.4	289	16.1	22.2
20	23.9	310	10.6	17.4
15	29.8	278	6.32	14.1
10	35.1	217	2.95	10.9
5	38.0	116	0.74	7.5

TABLE II

$$K_1 = -5500 \text{ ergs/cm}^3 \quad (14)$$

$$I_s = 1760 \text{ Gauss} \quad (14)$$

$$L = 0.88 \text{ mm}$$

sample thickness $= 0.20$ mm

exchange energy $= 4.4 \times 10^{-7}$ ergs/cm (15)

The intensity of domain magnetization parallel to the applied field is $I = I_s \cos \theta$. For the condition $\theta = 0$, $I = I_s$ and the sample is in the saturated condition. Table I therefore lists the computed results using the angle θ as the entering argument.

Table II lists the principal physical characteristics of the crystal sample.

Figure 10 is a plot of the computed domain spacing vs. applied magnetic field as listed in Table I.

5.3 Conclusions

That the experimental results sustain at least qualitatively the theoretical description of the phenomena can be seen by a comparison of figures 7 and 10. The predicted saturation point ($H = 40$ oersteds), is experimentally observed, and the general shape of the curves is the same. However d experimental varies from 5 to 2 times d predicted. This result is not unique in that several other experimenters (3) have had similar experience (i.e. $d_{observed} \cong 5 \ d_{predicted}$).

There are several possible explanations for this result. The most likely one is rooted in the simplifying approximation made earlier. A more complicated domain closure pattern than that postulated by figure 8(b)
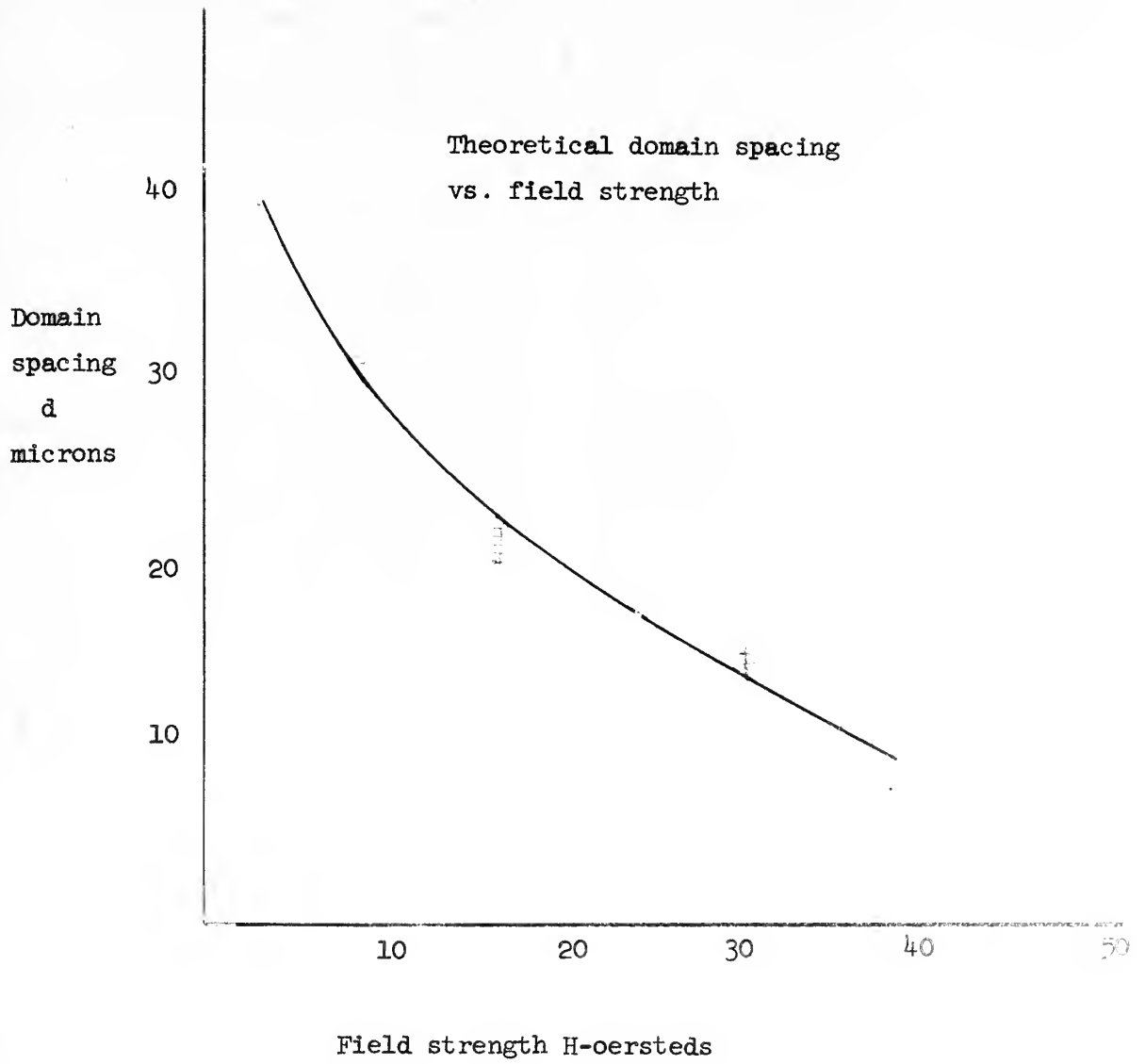
Figure 10 - Plot of theoretical domain spacing vs. theoretical applied field strength.

would possess less energy. Since $d \propto \dfrac{1}{(W_b)^{\frac{1}{2}}}$, the calculated domain

spacing for a more complicated closure system would be larger and would

therefore be in closer agreement with experimental results. Unfortunately,

no observations were made on the (100) plane face of the sample and

therefore no experimental verification of figure 8(c) patterns can be

made. However, Bates and Wilson (16) investigated the effects of

magnetic fields on the domain structure of nickel which has [111] as

its easy direction. Their results indicated that closure domains existed

both at the top and along the sides of a rectangular specimen, and tends

to support the contention concerning more complicated closures.

The conclusion of this discussion is certainly that the domain

hypothesis in ferrimagnetic media is substantiated by the evidence of

this experiment.

CHAPTER VI

MISCELLANEOUS EXPERIMENTAL OBSERVATIONS

6.1 Domain Structure Observed in a Toroid

As mentioned in Section IV, a toroid shaped specimen was cut in
the (110) plane of YIG. It was hoped that this geometry, when suitably
magnetized by passing current through a number of turns of wire through
the sample, would produce circular continuous walls.

Figure 11 illustrates the typical domain structures encountered. The
pattern is composed of many rectangular subsections distributed around
the surface of the sample. All the rectangular domains are oriented in
the same direction.

As the magnetic field was varied, motion of the rectangular walls
was observed. Because of the heat generation problem in the coils,
fields above approximately 20 oersteds created violent boiling of the
colloid and obliterated the wall structures. Figure 11 was photographed
at the zero field condition.

6.2 Patterns in a Rectangular Corner

Figure 12 captures an unusual effect detected at the corner of the
rectangular specimen subjected to high fields. One recalls that the
bulk of this specimen was essentially saturated in fields of approximately
40 oersteds. The ends of the sample however exhibited a more complicated
domain structure (figures 4, 5, and 6). In figure 12, one observes the
formation of a new domain wall as the field is increased. At $H = 84$ oersteds
the Bloch wall (white diagonal line) is moving down and to the right.
At $H = 85$ oersteds, the wall splits in its center. As the field is
increased the two sections move away from each other. This behavior tends
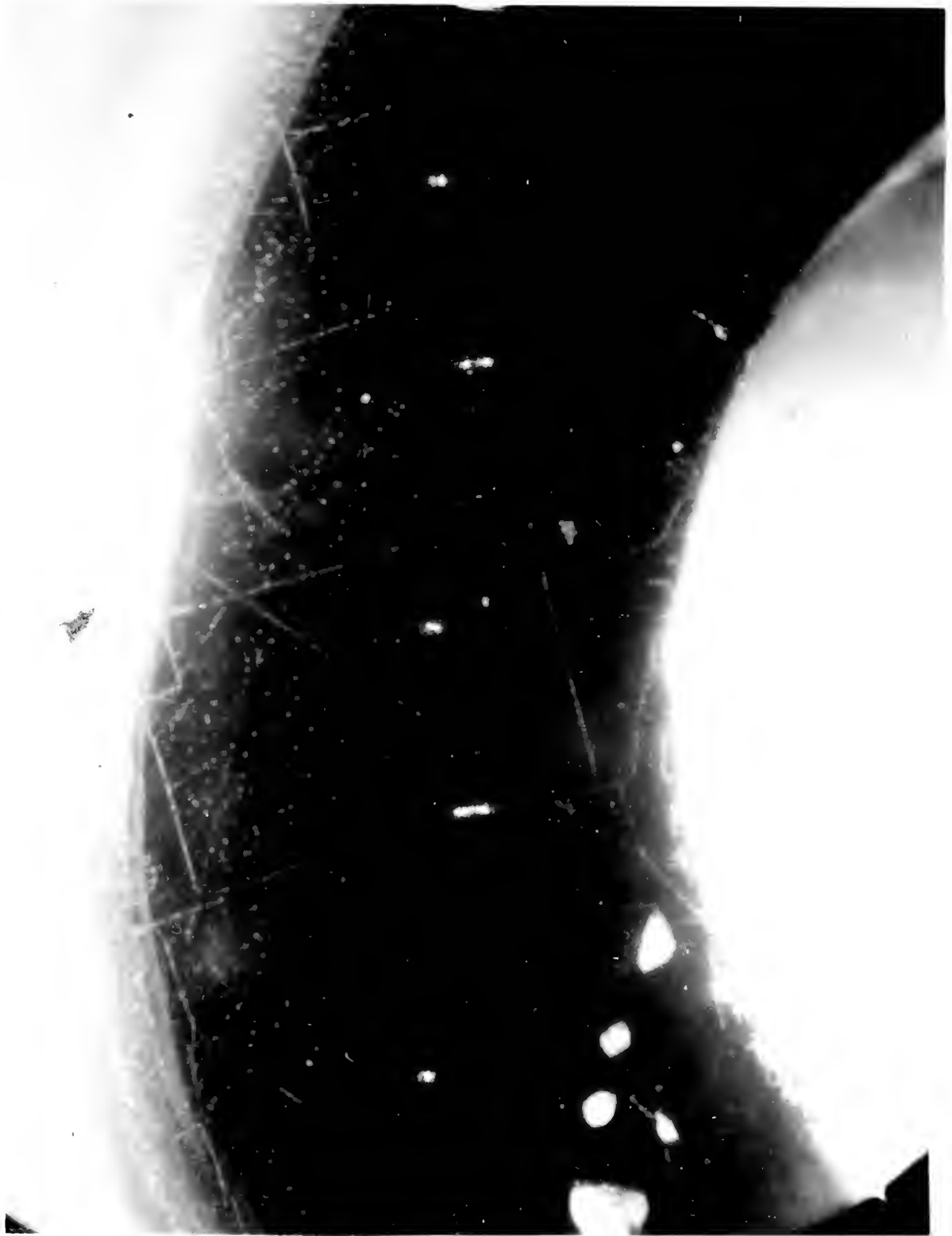to confirm the dependence of domain spacing on the width of a specimen.

FIGURE 11.

The phenomena illustrated by figure 12 was quite reproducable. As the field was varied continuously between 50 oersteds and 130 oersteds the observed domain structure cycled as described above.

6.3 Dry Powder Experiments

One of the more ambitious projects of this experiments was to observe domain structures at low temperature (approximately $80^{\circ}K$), and thereby study magnetic anneal effects in a single crystal sample. Considerable work has been done in this area by the Magnetics Group of the Laboratory for Insulation Research at M.I.T. utilizing polycrystalline samples.

Since the colloid suspension technique is good only in the vicinity of room temperature, the dry powder method of domain observation was attempted (7). The procedure was quite simple. The carefully prepared surface of the sample was gently dusted with extremely fine magnetic particles. In much the same manner as the colloid suspension, these particles are attracted to the Bloch walls. Antara Chemical of New York, New York, gratiously provided 3 micron carbonyl iron powders. These proved too large in that no detectable pattern was discernable.

Other investigators advised the use of iron penta carbonyl as a powder generating agent (17). In this procedure, liquid iron penta carbonyl is ignited. As it burns, it gives off a fine brown smoke which contains iron carbonyl particles less than 1 micron in diameter. The rectangular sample was inserted into a cloud of these particles. The results however were again discouraging. Domains appeared only at the edges of the sample though continuously around its entire circumference. They possessed the characteristic ribbon like structure much like those obtained with the colloid. However, the bulk of the specimen had no observable domain pattern.
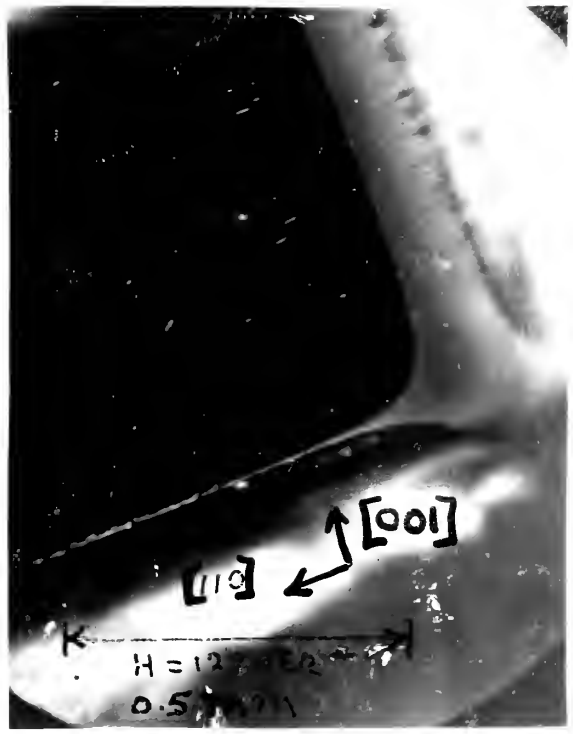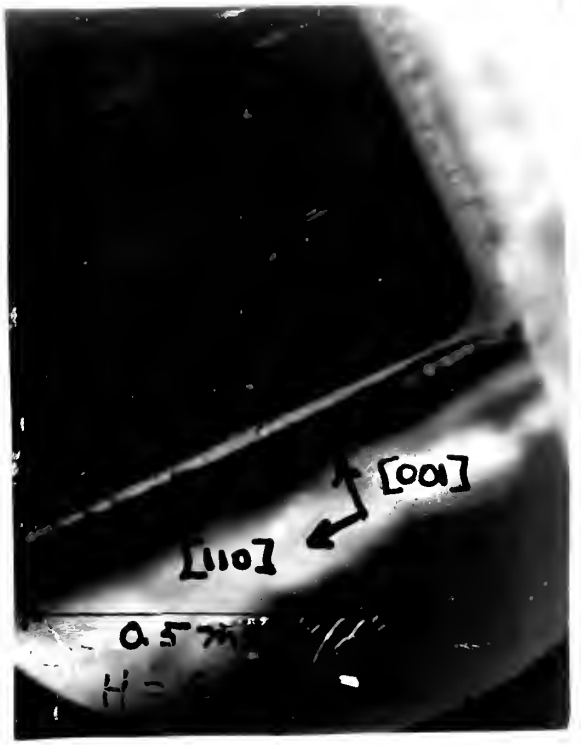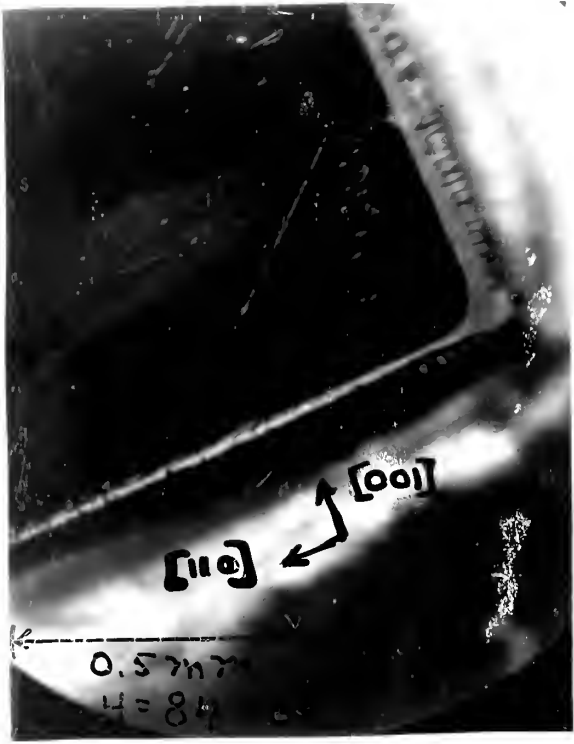
There are several possible reasons for such behavior. The major one seems to be the inherent lack of particle mobility with the dry powder method in conjunction with the low anisotropy (K_1 = -5500 ergs/cm^3) of the YIG sample. The appearance of domains at the edges of the sample was probably caused by the existing closure domain pattern. It was shown previously that closure patterns possess an excess energy over and above the energy density in the bulk of the material and would therefore tend to produce larger forces with which to attract the powder particles.

It is now felt that for visual observation of domain structure in YIG at low temperatures, one will, of necessity, have to shift to one of the other visual techniques such as those utilizing the Kerr Effect (7) or Faraday Rotation Effect (7). Such procedures are however much more complicated and expensive.

APPENDIX A

COLLOID PREPARATION

The colloidal suspension was prepared by Mr. Janis Kanajs
using the following method as suggested by Mr. D. Wickham of
Lincoln Laboratory.

The first part of the procedure is the same as that given by
Elmore in Phys. Rev. $\underline{54}$, 309 (1938), which is - dissolve 2 grams of
ferrous chloride ($FeCl_2$, $4H_2O$) and 5.4 grams of ferric chloride
($FeCl_3$, $6H_2O$) in 300 ml. of hot water and add to this with constant
stirring 5 grams of sodium hydroxide in 50 ml. of water. Then filter
to remove the excess salt and caustic and thoroughly wash the
precipitate. Filtering is very slow so it is best to centrifuge it
five or six times until there is a tendency for the material to stay
in suspension.

Then, instead of using a soap solution as Elmore did, a stabilizing
solution is made as follows: 2 g. of cocoanut oil amine (mostly
<u>dodecyl amine</u>, m.p. - $10^{o}C$) as prepared by Armour and Co. is added
to 10 cc, 1 N HCl to bring to pH 7. The solution is then diluted
with distilled water to 50 cc. total volume, and 20 cc. of the iron
oxide slurry is added. After thorough mixing it may be necessary to
add a drop of HCl to bring to pH 7. The whole system is then brought
up to 150 cc. with distilled water, and is stirred vigorously at
6000 rpm, for 20 min. It is finally diluted again to a total of
600 cc., and is ready for use. It should be pointed out that the
slurry should not be permitted to stand for any great length of time
before adding the stabilizing solution.

The use of the dodecylamine hydrochloride is due to W. O. Baker
and F. H. Winslow of the Bell Laboratories.

APPENDIX B

CRYSTAL GROWING PROCEDURE

The YIG crystals used in conjunction with this thesis were grown by R. Hunt (12). The exact method of growing the crystals is given in detail in R. Hunt's Ph.D. thesis of June, 1964 which is as yet unpublished.

Briefly the procedure is as follows. Appropriate weights of Y_2O_3, Fe_2O_3, PbO, and $PbFe_2$ are mixed in a blender with toluene. After mixing the toluene is partially removed by vacuum filtering and the mixture is allowed to dry completely. It is then packed into a crucible and inserted into a furnace at $1290^\circ C$ where it remains for 9 hours. It is then cooled at a rate of 2° per hour to $1025^\circ C$ and thence at 30° per hour.

This procedure produces very large single crystals of YIG.

APPENDIX C

Analytic Expressions to Describe the Observed Domain Structures

Using figures 1 and 9 in conjunction with expressions introduced in Chapter II for the magnetocrystalline energy and the energy in the applied field, the energy in the bulk of the sample is expressable as:

$$E_{bulk} = E_K + E_H$$

where

$$E_K = K_1(\alpha_1^2 \alpha_2^2 + \alpha_2^2 \alpha_3^2 + \alpha_1^2 \alpha_3^2)$$

$$E_H = - I_s H \cos \Theta$$

Also from figures 1 and 9 and by symmetry arguments:

$$\alpha_1 = \cos(90^\circ - \Theta) = \sin \Theta$$

$$\alpha_2^2 = \alpha_3^2 = \frac{1}{2} (1 - \alpha_1^2)$$

Use of these expressions lead to:

$$E_K = \frac{K_1}{4} (1 - \alpha_1^2) (1 + 3 \alpha_1^2)$$

$$E_K = \frac{K_1}{4} (1 + 2 \sin^2 \Theta - 3 \sin^4 \Theta)$$

Therefore, the bulk energy becomes:

$$E_{bulk} = \frac{K_1}{4} (1 + 2 \sin^2 \Theta - 3 \sin^4 \Theta) - HI_s \cos \Theta$$

for a minimum of E_{bulk},

$$\frac{d(E_K + E_H)}{d\Theta} = 0$$

and leads to the following results:

$$H = \frac{K_1}{I_s} \cos \Theta (3 \sin^2 \Theta - 1)$$

and

$$E_{bulk} = \frac{K_1}{4} (5 - 14 \sin^2 \Theta + 9 \sin^4 \Theta)$$

Néel (2,6) has developed a general expression for the wall energy in terms of the magnetocrystalline energy and the exchange energy. In terms defined in figure 13, the wall energy density is:

$$\gamma = \sin \beta \sqrt{\frac{2A}{3}} \int_{\Theta_1}^{\Theta_2} \sqrt{f(\Theta)} \; d\Theta \; ergs/cm^2$$

where β = smaller angle between domain magnetization and normal to the wall.

   A = Landau-Lifschitz exchange stiffness constant

   $f(\Theta) = E_K(\Theta) - E_K(\Theta = 0)$

For a complete derivation of the above expression see Néel's paper. The walls considered in this experiment are as shown in figure 13 and have the following in common:

a) Θ varies from 0° to 180° as the wall is entered traversed and excited.

b) β = constant through the wall.

The expression E_K, the magnetocrystalline energy, for a crystal in which a wall is normal to the   110   direction in terms of β and Θ of figure 13 is:

$$E_K = \frac{K_1}{4} \left[1 - 4 \sin^2 \beta + 4 \sin^4 \beta + (6 \sin^2\beta - 4 \sin^4\beta)\sin^2\Theta - 3 \sin^4 \beta \sin^4 \Theta \right]$$

$$f(\Theta) = E_K(\Theta) - E_K(\Theta = 0)$$

$$\left[f(\Theta) \right]^{1/2} = \frac{B}{2} \sqrt{K_1} \left[\sin \Theta (E^2 + \cos^2 \Theta)^{1/2} \right]$$

   where $B^2 = 3 \sin^4 \beta$
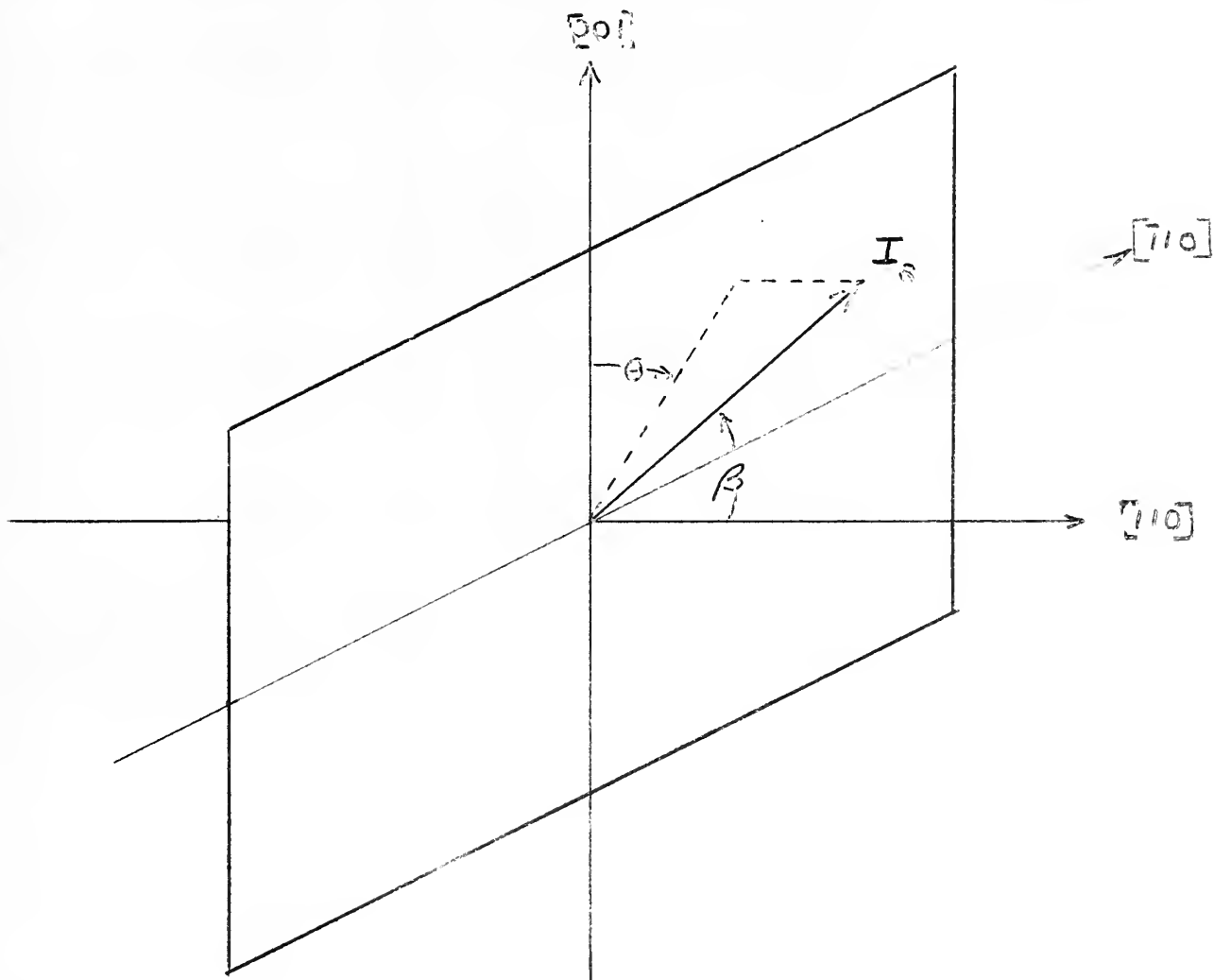
$$E^2 = \frac{6 - 7 \sin^2 \beta}{3 \sin^2 \beta}$$

Figure 13 - Reference directions for calculating wall energy
densities.

$$\gamma = \sin \beta \sqrt{\frac{2A}{3}} \int_{\Theta_1}^{\Theta_2} (f(\Theta))^{1/2} \, d\Theta$$

$$\gamma = \sin \beta \sqrt{\frac{2A}{3}} \int_{\Theta_1}^{\Theta_2} \frac{B}{2} \sqrt{K_1} \left[\sin \Theta (E^2 + \cos^2 \Theta)^{1/2} \right]$$

let $u = \cos \Theta$

$\quad du = - \sin \Theta \, d\Theta$

then

$$\gamma = - B \sin \beta \sqrt{\frac{AK_1}{6}} \int_0^\pi (E^2 + u^2)^{1/2} \, du$$

Carrying out the above integration and simplifying leads to the following expression for the wall energy density

$$\gamma = \sin \beta \sqrt{\frac{AK_1}{6}} \left\{ \sin \beta (6 - 4 \sin^2\beta) + \frac{6 - 7\sin^2 B}{\sqrt{3}} \sinh^{-1} \sqrt{\frac{3\sin^2\beta}{6 - 7\sin^2\beta}} \right\}$$

APPENDIX D

BIBLIOGRAPHY

1. Bitter, F., _Phys. Rev._, Vol. 38, 1931, pp. 1903.

2. Néel, L., _J. Phys. Radium_, Vol. 5, 1944, pp. 241.

3. Stewart, K.H., _Ferromagnetic Domains_, University Press, Cambridge, G.B., 1954.

4. Akulov, N.S., _Z. Phys._, Vol. 69, 1931, pp. 78.

5. Kittel, C., _Rev. of Mod. Phys._, Vol. 21, Oct. 1949, pp. 541.

6. Néel, L., _Cah. Phys._, Vol. 25, 1944, pp. 1.

7. _Magnetism_, Rado, G.T. and Suhl, H., eds., Vol. 3, pp. 415, Academic Press, New York, N.Y., 1963.

8. Elmore, W.C., _Phys. Rev._, Vol. 54, 1938, pp. 1092.

9. _The Crystalline State_, 3 V., Bragg, W.H., ed., Vol. 1, Bradford and Dickens, London, 1955.

10. Williams, H.J., Bozorth, R.M., and Shockley, W., _Phys. Rev._, Vol. 25, 1949, pp. 155.

11. Yamamoto, M. and Iwata, T., _Phys. Rev._, Vol. 81, 1951, pp. 887.

12. Williams, H.J. and Walker, J.G., _Phys. Rev._, Vol. 83, 1951, pp. 634.

13. _Solid State Physics_, Seitz, F. and Turnbull, D., eds., Vol. 3, pp. 439, Academic Press, New York, N.Y., 1956.

14. Hunt, R., MIT Ph.D. thesis, June, 1964 (unpublished).

15. Kunzler, J.E., Walker, L.R. and Galt, J.K., _Phys. Rev._, Vol. 119, 1960, pp. 1609.

16. Bates, L. and Williams, G., _Proc. Phys. Soc._ (London), Vol. A64, 1951, pp. 691.

17. Andra, W. and Schwabe, E., _Ann. Physik_, Vol. 17, 1955, pp. 55.

18. Bozorth, R.M., _Ferromagnetism_, New York, N.Y., 1951, Van Nostrand.

19. Craik, D.J. and Tebble, R.S., <u>Reports on Progress in Physics</u>, Vol. 24, 1961, pp. 116.

20. Dillon, J.F. and Earl, H.E., <u>Amer. J. of Phys</u>., Vol. 27, April 1959, pp. 201.

21. Bates, J.F. and Hart, A., <u>Proc. Phys. Soc</u>. (London), Vol. B69, 1956, pp. 497.

22. Elmore, W.C., <u>Phys. Rev</u>., Vol. 62, 1942, pp. 406.